# Amphiphilic Cellulose as Stabilizer for Oil/Water Emulsion

M. El-Sakhawy[1*], S. Kamel[1], A. Salama[1], M. A. Youssef[2], Wafia Elsaid Teyor[2] and Hebat-Allah S. Tohamy[1]
[1] Cellulose and Paper Department, National Research Centre, 33 El-Bohouth St. (former El-Tahrir st.), Dokki Giza, P. O. 12622.[2] Department of Chemistry, Faculty of Science, Helwan University, Egypt.

IN THIS work, amphiphilic ethyl amino-cellulose as oil/water emulsion stabilizer was prepared from cellulose extracted from bleached bagasse pulp. By periodate oxidation of cellulose the corresponding C-2/C-3 dialdehyde cellulose produced, which reacted with ethyl amine to obtain ethyl amino-cellulose (amphiphilic cellulose) through Schiff's base reaction (reductive amination). The produced ethyl-amino cellulose has a great attention in soybean oil/water stabilization. The amphiphilic cellulose was characterized by Fourier transform infrared spectroscopy (FTIR), X-ray diffraction, Transmission electron microscopy (TEM), Thermal gravimetric analysis (TGA), and Differential scanning calorimetry (DSC). Fourier transform infrared spectroscopy has been proved the incorporation of soybean oil in ethyl amino-cellulose as there is new groups appeared in the Fourier transform infrared spectra of the prepared emulsion. TEM was used to prove the nano-size of the prepared samples. TGA and DSC proved the thermal stability and melting temperature. The prepared sample was successfully applied as a stabilizer for soybean oil in water emulsion.

Keywords: Amphiphilic polymers, Periodate oxidation, Amino-functionalization, Soybean oil /water emulsion.
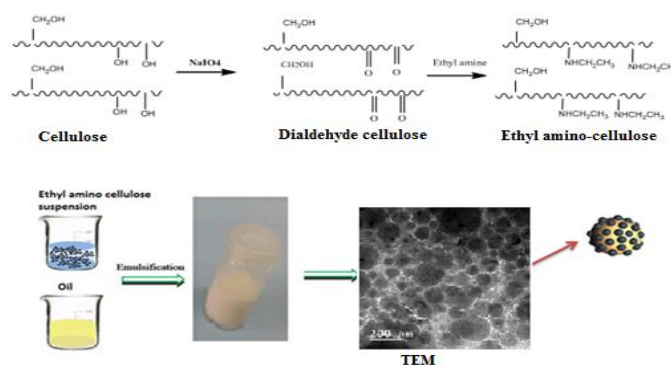
M.El-Sakhawy *et al.*

Amphiphiles are polymeric materials with hydrophobic and hydrophilic moieties. Their hydrophobicity originates from a pendant side chain. They are applied in various applications such as emulsion stabilizers in the aqueous phase. They can also have stimuli-response properties, such as pH and temperature sensitivity. A number of naturally occurring polysaccharides, such as Arabic gum, pectin, and, chitosan are capable of stabilizing emulsions [1]. Natural cellulose and starches are not considered as amphiphiles. Chemical modifications are made on cellulose and starches to introduce surface active groups. Starches are essentially hydrophilic molecules with poor surface activity, whereas cellulose is hydrophilic, but it is insoluble in water because of strong intermolecular H-bonds [2].

It is known that; cellulose is the most widespread polymeric raw material in nature. It is obtained from different plants and bacterial sources. It has attracted attention as one of the most promising polysaccharides for accomplishing NPs [3]. Periodate utilization as an oxidizing agent precedes an important method for functionalization of the two secondary OH groups in cellulose in order to obtain 2, 3-dialdehyde cellulose (DAC) [3,4].

DAC is biodegradable and biocompatible. CHO groups of DAC can be further reacted with an amine (reductive amination) by the Schiff base reaction introducing an imine bond between the amine and cellulose [5]. Reductive amination of DAC is used to produce amphiphilic amino cellulose [6]. Due to numerous properties of DAC, there has been an interest in alkylation of cellulose with amine chains via modification reactions such as reductive amination [7]. In this method, the amine first condenses with a carbonyl group of the aldehyde group to give an imine through Schiff base reaction. A reducing agent, such as $NaBH_4$ reduces the imine to give the amine product. The reaction is best carried out under mildly acidic conditions [8].

The Schiff base forming reaction between primary alkyl amine (*e.g.* ethyl amine) and CHO group of DAC is a useful procedure to give nitrogen containing derivatives [7,9].

Amphiphilic amino cellulose has been used as effective stabilizer with O/W emulsions [6].

The purpose of the present work is to utilize periodate oxidation approach in order to incorporate primary amine compounds to DAC surfaces via Schiff's base reaction which in turn used as a stabilizer for soybean oil in water emulsion.

Experimental

Sugar cane bagasse delivered from Quena Paper Industry Company, Egypt. Acetic acid 96%, glacial acetic acid, sodium periodate, absolute ethyl alcohol,

diethyl ether, acetone, ethyl amine, sodium borohydride and other chemicals were of pure analytical grades and used without further modification.

Preparation of cellulose from sugarcane bagasse (SCB)

SCB was hydrolyzed with 1.5% HCl, based on the raw material, using liquor to material ratio of 1:10 at 120 ºC for 2 hr. The prehydrolyzed bagasse was treated with 20% NaOH (based on SCB) using liquor to material ratio of 1:7 at 170 ºC for 2 hr. Residual lignin of pretreated bagasse was removed by bleaching with sodium chlorite. Mercerization of cellulose was carried out by 17.5% NaOH to remove the traces of lignin and other constituents. The chemical composition of the obtained pulp was comprised from α-Cellulose 94.2%, Lignin 0.3%, Hemi-cellulose 3.4%, and Ash 0.4%.

Characterization of the lignocellulosic material

The yield and the percentage chemical constituents such as ash, lignin content and α-cellulose were determined according to the standard methods [10].

Synthesis of dialdehyde cellulose (DAC)

DAC was synthesized according to the procedure described by Sirvio with little modification [5]. In brief, DAC was prepared by oxidizing 1 g of cellulose using (0.2, 0.4, 0.8 g) of sodium periodate as an oxidant (designated as DAC_1, DAC_2 and DAC_3 respectively) in 50 ml distilled water and a reaction vessel was covered with an aluminum foil to prevent the photo-induced decomposition of periodate. The reaction mixture was stirred with a magnetic stirrer in a water bath at 70 ºC for 3h. After washing with deionized water (2000 ml), DAC was stored in a non-dried state at 4 ºC.

Determination of aldehyde content in DAC

The determination of aldehyde content, degree of oxidation (D.O.), of DAC was based on the reaction between aldehyde group and the hydroxyl amine hydrochloride (Scheme 1). The never-dried periodate oxidized cellulose (0.1 g) was placed in a 250 ml beaker containing 25 ml of 0.25 M hydroxyl amine hydrochloride. The beaker was covered with aluminum foil and the mixture was stirred 48 hr. at room temperature with a magnetic stirrer [4]. Product was filtrated and washed with 600 ml of deionized water after which it was dried. Nitrogen content of the oxime derivative of DAC was determined by using a Vario El Elementar CHNS/O elemental analyzer [5].

As illustrated in Scheme 1, 1 mol of aldehyde reacts with 1 mol of hydroxyl amine hydrochloride and the aldehyde content can be calculated directly from nitrogen content of the product [5].

0.25 M hydroxylamine hydrochloride-solution was prepared by first dissolving 17.55 g hydroxyl amine hydrochloride (99%) in 150 ml of water. The solution was then diluted to 1 liter and pH was adjusted to 4.0 with 0.1 M NaOH [4].

M.El-Sakhawy *et al.*
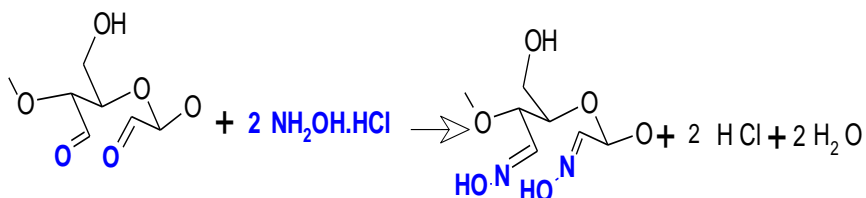
Scheme 1. Degree of oxidation determination.

Preparation of amphiphilic ethyl amino-cellulose (EAC)

EAC was prepared according to the procedure described by Visanko with little modification [6]. First, $DAC_{1, 2, 3}$ fibers (9 g in 900 ml deionized water) were acidified with a dilute HCl (1%), pH= 4.5 , stirring for 15 min, then ethyl amine (10.05 ml) and sodium borohydride (3.544 g) were mixed. The reaction was continued for 72 hr. under magnetic stirring in a closed container at room temperature. The product was precipitated first with excess ethanol or ethyl acetate, centrifuged and finally washed with water until neutrality. The amino group content of $EAC_{1, 2, 3}$ was determined using an elemental analyzer by measuring the nitrogen content of the dried sample.

Ethyl amino-cellulose as stabilizer in O/W emulsion

The performance of amphiphilic EAC as stabilizers in O/W emulsions was investigated by using $EAC_{1, 2, 3}$ (0.5 g) was mixed with water (1.5 ml). Soybean oil (200) was added by mixing with an Ultra/sonicator for 3 min in ice. The reference O/W emulsion was fabricated by mixing deionized water (1.5 ml) and soybean oil (200μ). The stability of the ethyl amino-cellulose treated O/W emulsions was evaluated with TEM by measuring the average particle size of the oil droplets [6].

Characterization
Fourier transform infrared spectroscopy (FTIR).

Infrared spectra were recorded with a JASCO FT/IR, Nicolet, Model 670 in the region from 4000 to 400cm^{-1}.

X-ray Diffractions (XRD)

The crystallinity was analyzed using X-ray diffraction. Diffraction patterns were obtained using a Brukur D8 Advance X-ray diffractometer (Germany). The diffraction patterns were recorded at a voltage of 40 kV with a current of 40 mA using copper (Kα) radiation (1.5406 Å). Specimens were prepared from cellulose or cellulose derivatives by pressing tablets with a thickness of 1 mm after freeze-drying the samples. Scans were taken over a 2θ (Bragg angle) range from 5 to 80°. The degree of crystallinity in terms of the crystallinity index (CrI) was calculated as follows:

$$Cr.I. (\%) = (Sc / St) \cdot 100$$

where: Sc is area of the crystalline domain; St is area of the total domain [11].

The change of crystallinity calculated as follows [12]:

$$\Delta CrI\% = \frac{(CrI)modified\ cellulose - (CrI)pure\ cellulose}{(CrI)pure\ cellulose} * 100$$

Elemental analysis

Via Vario El Elementar was used, to obtain the percentage of C, N, H, S, O.

Transmission Electron Microscope (TEM)

The morphological features of the fabricated DAC and EAC were analyzed with transmission electron microscope. Samples were prepared by diluting each sample with 1ml distilled water. A small droplet of the dilution was dosed on top of a carbon-coated and glow-discharged copper grid. Grids were dried in room temperature and analyzed under standard conditions.

Thermogravimetric Analysis (TGA)

The TGA studies were carried out on the samples powder by using Perkin Elmer thermogravimetric analyzer with nitrogen as purge gas. Specimen, approximately 4.876 mg, were loaded into platinum TGA pans and ramped from room temperature to 600°C at heating rate of 10°C/min in nitrogen atmosphere.

Differential Scanning Calorimetry (DSC)

Thermal scans were performed using TA Instruments SDT Q600 V20.9 equipment. Dry N_2 was used as the purge gas. Specimens were heated at rates of 10 °C/min, in the temperature range from room temperature to 600ºC.

Results and Discussion

Characterization of dialdehyde cellulose (DAC)

Cellulose was extracted from bagasse by acid hydrolysis followed by soda extraction and then bleached with sodium chlorite giving pulp with 94.2% α-cellulose. Oxidations by sodium periodate yields the corresponding C-2/C-3 $DAC_{1,\ 2,\ 3}$. Table 1 shows the aldehyde content and degree of oxidation (D.O.) of DAC based on the N% consistence after oxime reaction. The effect of $NaIO_4$ amount on the aldehyde content of DAC is shown in Table 2. It was shown that the aldehyde content increased with the increasing of $NaIO_4$ dosage.

Characterization of ethyl amino-cellulose (EAC)

Periodate oxidation is a well-known reaction that results in the formation of DAC by opening the anhydroglucose unit (AGU) of cellulose. According to the

equilibrium reaction equation, one mole of $NaIO_4$ is consumed per one mole of AGU, resulting in the formation of two moles of aldehyde groups. The obtained aldehyde groups have a different reactivity than their parent hydroxyl groups, allowing them to be modified by amination in which aldehyde first reacts with amine to form imine, followed by reduction to a secondary amine. DAC_3 with aldehyde group content of 5.98 mmol/g (DAC_3) was then reacted with ethyl amine to obtain ethyl amino-cellulose (EAC_3). The schematic pathway for $NaIO_4$ oxidation and amination of cellulose is shown in Scheme 2.
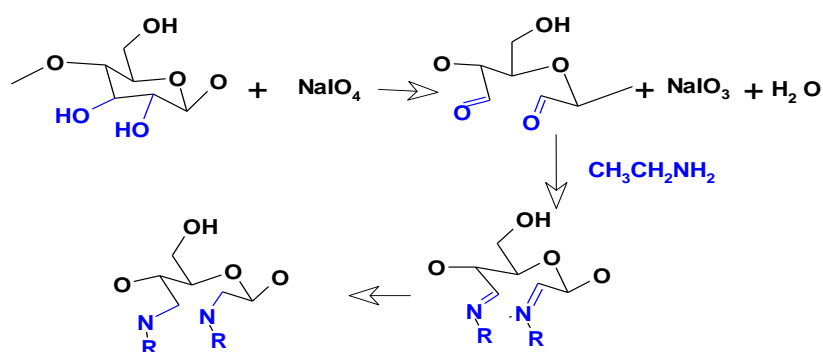
Scheme 2. $NaIO_4$ oxidation and reductive amination of cellulose, R= CH_2-CH_3.

According to nitrogen content the calculated DS of the prepared EAC samples are listed in Table 3 [13].

Based on the elemental analysis of N%, Table 3 shows that only 8−19% of the aldehyde groups were converted to ethyl amine derivative; therefore, it can be assumed that the rest of the aldehydes were reduced to hydroxyl groups by sodium borohydride, which is reported as reducing agent of imine in the presence of aldehyde.

The low reaction efficiency might be due to the low formation rate of imine in the aqueous environment [13].

TABLE 1. Nitrogen consistence and degree of oxidation of oxime's dialdehyde cellulose derivatives.

Sample	Nitrogen consistence	D.O. (mmol/g)
	N (%)	
Oxime's DAC_1 derivative	2.643	1.89
Oxime's DAC_2 derivative	3.979	2.84
Oxime's DAC_3 derivative	8.374	5.98

TABLE 2. Effects of sodium periodate concentration on the aldehyde content.

Sample Code	DAC_1	DAC_2	DAC_3
$NaIO_4$ /Cellulose (mol/mol)	0.15	0.30	0.60
Aldehyde content (mmol/g)	1.89	2.84	5.98

TABLE 3. Nitrogen consistence and degree of substitution of ethyl amino-cellulose derivatives.

Sample	Nitrogen consistence	DS (mmol/g)
	N (%)	
EAC_1	0.51	0.36
EAC_2	0.654	0.47
EAC_3	0.728	0.52

FT-IR spectra

Figure1 Exhibits the FT-IR spectra of cellulose, DAC_3 and EAC_3. Cellulose showed characteristic bands at 3482.81, 2897.52, 1370.18, 1034.62 and 898.666 cm^{-1} which related to O-H stretching, C-H stretching, C-H bending, C-O-C pyranose ring viberation and glycosidic linkage between glucose units in cellulose respectively.
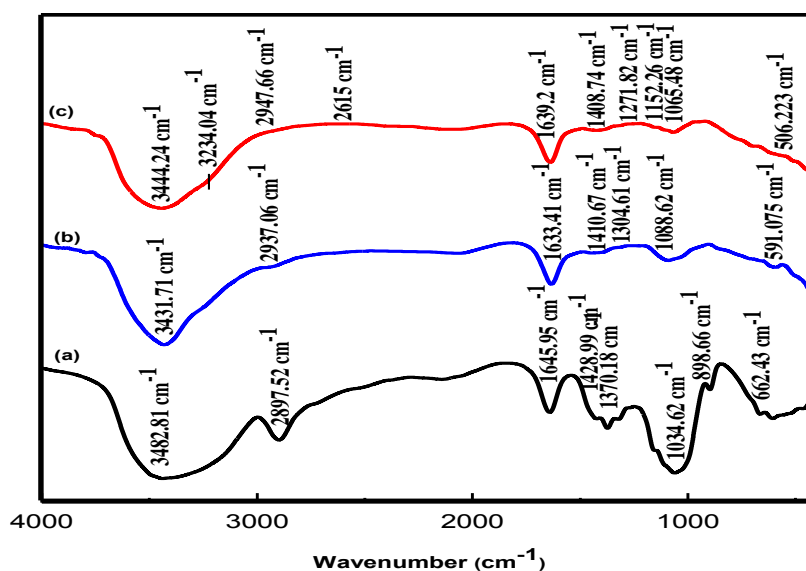
Fig. 1. FT-IR spectra of (a) cellulose; (b) dialdehyde cellulose (DAC$_3$) and (c) ethyl amino-cellulose (EAC$_3$).

Compared with the spectrum of unmodified cellulose, two new absorption bands at around 1633 and 1088 cm^{-1} appeared in the spectrum of DAC$_3$, corresponding to the characteristic absorption peaks of the aldehyde group (C=O) and hemiacetal bonds between newly achieved aldehyde groups and their neighboring hydroxyl groups (or water) at the same time, respectively. This result proved that the hydroxyl groups on the molecular chain of unmodified cellulose were partially oxidized to aldehyde groups, resulting in DAC [14,15].

The characteristic band of C-O-C became weak after oxidation. This tended to indicate a partial decomposition of cellulose during sodium periodate treatment [14.15].

The bands at 1633 related to C=O and 1088 cm^{-1}, related to hemiacetal were absent in the spectrum of EAC$_3$, which supported the successful reaction of DAC$_3$ with ethyl amine. FT-IR spectra of EAC$_3$ gave a new adsorption band at 3234 and 1639 cm^{-1}. This was corresponded to N–H stretching and bending vibration respectively, indicating successful amination-reduction reaction between the carbonyl and amine groups [3,13,14].

EAC$_3$ gave a new adsorption band at 1152 cm^{-1}, related to C- N stretching, which indicating the formation of a secondary amine bond on the cellulose (Fig. 1, Table 6) [13].

Absorption peak at 3444 cm^{-1} attributed to the OH stretching, which overlaps the NH stretching in the same region [15].

The introduction of two member chains (ethyl) is further confirmed by appearing additional peak of methylene (–CH$_2$-) stretching at 2615 cm^{-1}.

TABLE 4. Characteristic Bbands of the IR spectra of cellulose.

Wavenumber (cm^{-1})	Assignment	Relative absorbance
3482	A strong hydrogen- bonded O-H stretching vibration.	3.59
2897	C-H stretching.	1.74
1645	O-H bending from absorbed water.	1
1428	CH$_2$ bending of pyranose ring.	2.12
1370	C-H bending.	2.56
1034	C-O-C pyranose ring vibration.	2.42
898	β − Glycosidic linkage between glucose units in cellulose.	1.08

662	O-H out of plane bending.	2.07

TABLE 5. Characteristic bands of the IR spectra of dialdehyde cellulose.

Wavenumber (cm^{-1})	Assignment	Relative absorbance
3431	O-H stretching vibration.	2.53
2937	C-H stretching.	0.59
1633	C=O group.	1
1410	CH_2 bending of pyranose ring.	0.27
1304	C-H bending.	0.11
1088	Hemiacetal bonds plus C-O-C pyranose ring vibration.	0.44
591	β -Glycosidic linkage between glucose units in cellulose.	0.6

TABLE 6. Characteristic bands of the IR spectra of ethyl amino-cellulose.

Wavenumber (cm^{-1})	Assignment	Relative absorbance
3444	O-H stretching.	2.35
3234	N-H stretching vibration.	1.54
2947	C-H stretching.	0.25
2615	Methylene CH_2 of ethyl amine.	0.079
1639	N-H bending vibration.	1
1408	CH_2 bending of pyranose ring.	0.21
1271	-CH bending (CH_3) of ethyl amine.	0.08
1152	C-N stretching.	0.15
1065	C-O-C pyranose ring vibration.	0.27
506	β -Glycosidic linkage between glucose units in cellulose.	0.97

H-bonded OH stretching vibration of cellulose appeared at 3482 cm^{-1} was shifted to lower frequency at 3431 and 3444 cm^{-1} for DAC_3 and EAC_3 respectively. CH stretching mode appeared at 2897 cm^{-1} for cellulose was shifted to higher frequency at 2937 and 2947 cm^{-1} for DAC_3 and EAC_3 respectively. The change of the absorbance value of OH stretching vibration may be due to intermolecular hydrogen bonding [16].

TABLE 7. Crystallinity index and mean hydrogen bond strength of different samples.

Sample	CrI A_{1425} / A_{900}	MHBS (A_{OH}/A_{CH})
Cellulose	1.96	2.06
DAC_3	0.45	4.29

M.El-Sakhawy *et al.*

EAC$_3$	0.22	6.15

The relative absorbance of the bands corresponding to OH group in the region 4000-3000 cm^{-1} for spectra of cellulose was higher than DAC$_3$ and EAC$_3$ respectively.

According to El-Saied *et al.* [17] this change of band relative intensity indicates that the number of OH groups participating in H-bonds was higher in cellulose than in DAC$_3$ and EAC$_3$ respectively [17]. The increase of OH group relative intensity causes an increase in the CrI. This is due to the increase of the chance of formation of hydrogen bonds by increasing the OH groups. The rate of the decrease in CrI of EAC$_3$ is higher than DAC$_3$. This is due to the occupation of some of the OH groups and consequently the formation of hydrogen bonds decreases [18].

However there was no conformity between the data of crystallinity and mean hydrogen bond strength (MHBS). This was probably due to the type (intra- and inter-molecular) and degree of H-bonding formed.

Introducing amino groups onto DAC gives them potential affinity for two different phases as the ethylamine groups possess hydrophobic characteristics, while the cellulosic backbone remains hydrophilic. Therefore, EAC$_3$ was tested as potential stabilizers in O/W emulsions. The stabilizing effect of EAC$_3$ was evaluated with TEM. Figure 2 shows the dispersions of soybean oil in water, this figure shown the fully dispersion of oil in water after addition of EAC$_3$.
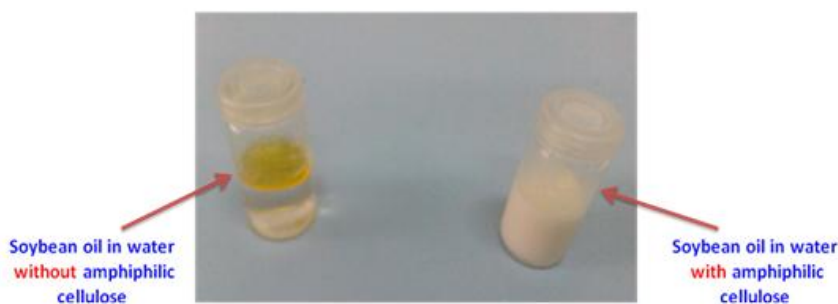

Soybean oil in water without amphiphilic cellulose

Soybean oil in water with amphiphilic cellulose

Fig. 2. Stability of soybean oil-in-water emulsion with ethyl amino-cellulose.

As observed in the FT-IR spectra (Fig. 3), the presence of N–H stretching and bending vibration at 3752 and 1639 cm^{-1} are the characteristic bands that confirm the presence of EAC$_3$. As observed in the FT-IR spectra, the introduction of long fatty acids member chains of soybean oil is further confirmed by the strong peaks at 2927 and 2857 cm^{-1} (assigned to C-H of CH$_3$ and –CH$_2$– stretching of methylene) which there relative absorbance is higher

than that of EAC_3. This shows that long aliphatic chains of oil were introduced to EAC_3 (Table 8) [7].
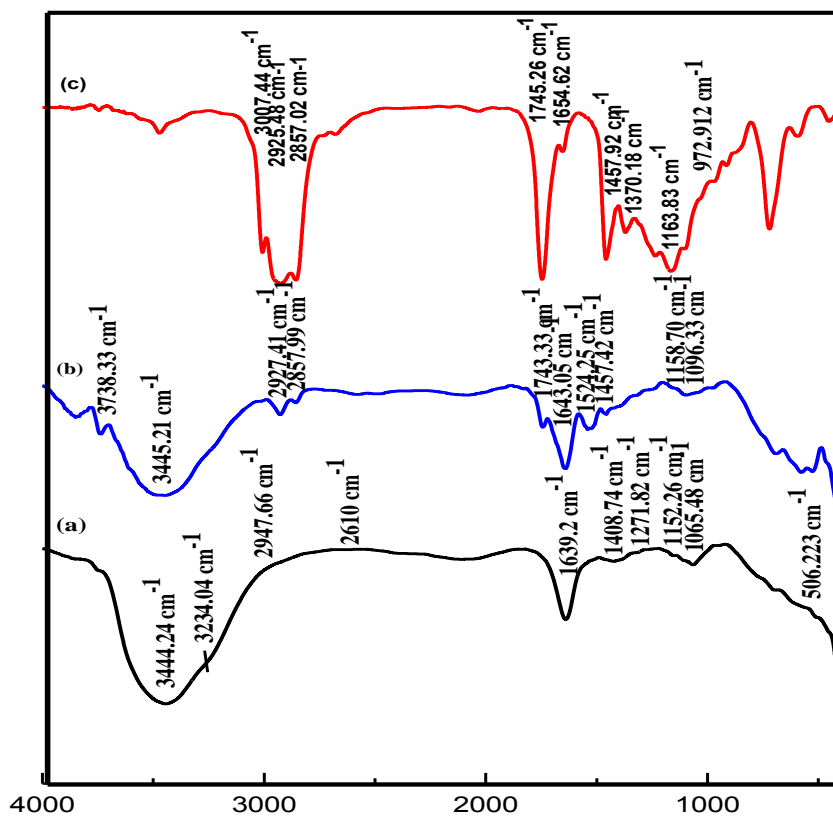

Fig. 3. FT-IR spectra of (a) ethyl amino-cellulose; (b) soybean oil and (c) oil/ water emulsion with ethyl-amino cellulose.

TABLE 8. Characteristic bands of the IR spectra of soybean oil [19].

Wavenumber (cm^{-1})	Assignment	Relative absorbance
3007	=C-H stretching.	5.19
2925	Methyl C-H stretching.	9.45
2857	Methylene CH_2 stretching.	8.67
1745	Asymmetric stretching vibration of C=O group.	8.50
1654	C=C stretching.	1
1457	CH_2 bending plus symmetric stretching vibration of C-O carboxylate group.	5.79
1370	-CH bending (CH_3).	3.88

| 972 | CH=CH bending out of plane. | 1.81 |

The introduction of oil can be proved also by the appearance of asymmetric and symmetric stretching vibration of carboxylate group (C=O, C-O) of soybean oil at 1743 and 1524 cm^{-1}. Also, the relative absorbance of C-H stretching (CH$_3$) and methylene (CH$_2$) stretching (0.25 and 0.20 respectively) for EAC$_3$ at 2947 and 2110 cm^{-1} respectively are lower than that of O/W emulsion with EAC$_3$ at 2947 and 2615 cm^{-1} (0.25 and 0.079 respectively).

In the case of O/W emulsion with EAC$_3$, spectra revealed that the relative absorbance of peaks dominated by soybean oil at 2925, 2857, 1745, 1654, and 1457 cm^{-1} decrease, confirming the incorporation of oil into EAC$_3$ emulsion during the formation of O/W emulsion with EAC$_3$.

The results from FT-IR spectra support the sequence of changes that occurred during the reaction stages.

Morphological investigation

The morphology of samples was portrayed with TEM, and the resulted images were analyzed with TEM image analysis software to evaluate the average size.

The particle size distributions of oil emulsified in water in the presence of EAC$_3$ was measured using TEM (Fig. 4). The mean particle size was found to be 47.44, 38.80, 921 and 194 nm of DAC$_3$, EAC$_3$, O/W without EAC$_3$, and soybean oil–EAC$_3$ emulsion respectively.

According to the TEM images EAC$_3$ appear as spherical-like shape instead of large clusters having a more uniform shape and size as in O/W suspension. As shown in Fig. 4, EAC$_3$ stabilizes the O/W emulsions most efficiently by decreasing the average particle size from 921nm to around 194 nm. The results showed that oxidized cellulose size is in nano range ($\approx$ 47.44 nm) meanwhile, EAC$_3$ size ($\approx$ 38.8 nm), this prove that size reduced after reductive amination.

The mechanism behind size reduction of EAC$_3$ is assumed to be resulting of multiple factors since NaIO$_4$ oxidation starts to shorten the ratio of the cellulose fibers. The transformation of OH groups to CHO groups in the neighboring positions of 2 and 3 is suspected to occur easily in the more reactive amorphous parts and less easily in the crystalline regions. The amorphous regions can be exposed to more chemical attack causing it to firstly dissolve from the surface of the cellulose fibrils. While the surface dissolves, the chemicals react further toward the core of the amorphous regions making its fail.

From Fig. 4 it is clear that, the periodate oxidation was not sufficient enough to liberate the cellulose NPs without the functionalization of CHO groups with amines to reduce cohesion within the cellulose structure. So, the reductive amination is the

key element for liberating individual cellulose NPs. This takes place by solubilising the cellulose chains from the weakened amorphous regions [6].

Particle size ≈ 47.44 *nm*   **Particle size ≈ 38.80 *nm***

Particle size ≈ *921.0 nm*   **Particle size ≈ 194.0 *nm***
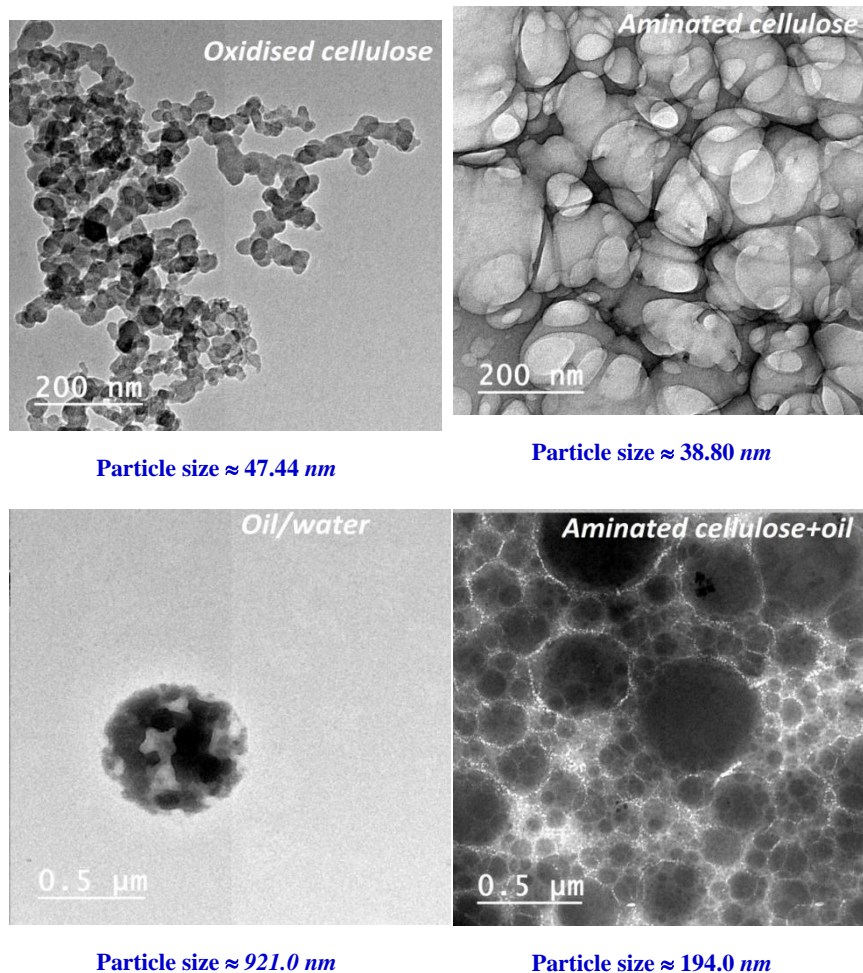
Fig. 4. TEM of oxidized cellulose (DAC₃); ethyl amino cellulose (aminated cellulose, assigned as EAC₃); oil in water (O/W) and oil in water with ethyl amino cellulose emulsion.

X-ray diffraction

   X-ray diffraction patterns of cellulose, DAC$_3$, and EAC$_3$ are presented in Fig. 5. The diffraction patterns show the characteristic peaks for cellulose II indicating that rearrangement of cellulose amorphous part takes place due to oxidation [15]. The crystallinity indexes calculated for cellulose, DAC$_3$, and EAC$_3$ were 61.02, 25.2, and 14.26%, respectively.
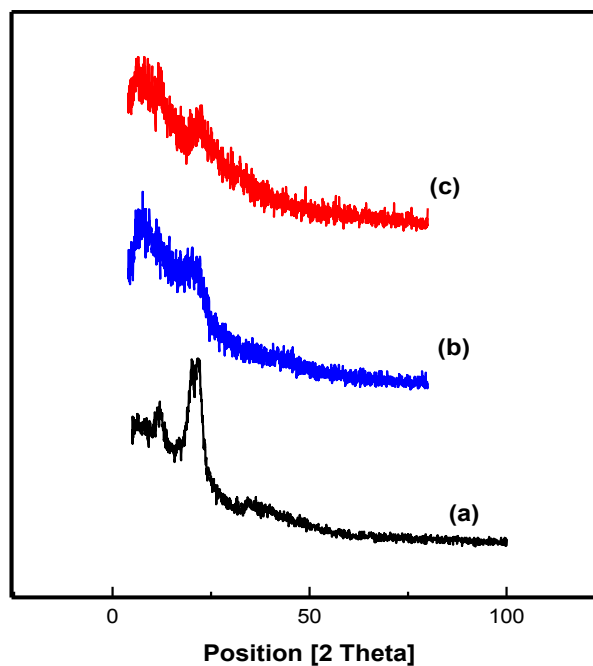
Fig. 5. X-ray diffrication of (a) cellulose; (b) dialdehyde cellulose (DAC₃) and (c) ethyl amino-cellulose (EAC₃).

TABLE 9. Characteristic bands of the IR spectra of oil/water emulsion with ethyl amino-cellulose.

Wavenumber (cm^{-1})	Assignment	Relative absorbance
3738	O-H stretching.	0.60
3445	N-H stretching vibration.	1.32
2927	C-H stretching.	0.38
2857	Methylene CH_2.	0.25
1743	Asymmetric stretching vibration of C=O carboxylate group.	0.52, 1
1643	N-H bending vibration plus C=C stretching.	1
1524	CH_2 bending of pyranose ring and fatty acid plus symmetric stretching vibration of C-O carboxylate group.	0.54

TABLE 10. Crystallinity of the prepared samples.

Sample	CrI%	ΔCrI%
Cellulose II	61.02	-
DAC_3	25.20	-58.7
EAC_3	14.26	-76.6

Thermal analysis of cellulose

Thermogravimetric analysis (TGA) and differential thermogravimetric analysis (DTA) of the prepared cellulose II, DAC_3 and EAC_3

The thermal decomposition process of cellulose and EAC_3 could be divided into two major reaction steps where a first weight loss of adsorbed water at 60.67 and 63.49°C respectively. The weight loss in the first step is higher for EAC_3 due to the sample was viscous and not dried (saved at 4 °C).

This initial weight loss is followed by the main final decomposition step at 353.34 and 92.71°C (accounting for a weight loss of 75.54 and 65.20%) for cellulose and EAC_3 respectively.

The 2nd weight loss may be related to decarboxylation and decomposition of cellulose, it includes dehydration, rearrangement, formation of carboxyl and carbonyl groups, evolution of CO_2 and CO and formation of carbonaceous char. This stage is known as volatilization or decomposition stage [20].

DAC_3 could be divided into four major reaction steps. The first step up to 65.67 °C (average weight loss 15.49%), assigned to adsorbed moisture.

The shape of thermogram curves changes only in the case of DAC_3. The 2nd degradation stage (referred to decomposition of cellulose) splits into two stages with the peak maxima 217.89 and 327.40 °C respectively with the total activation energy 38.54 kJ/mole, which indicates the lower thermal stability of DAC_3 than cellulose and $CMC_{0.45}$ (activation energy 95.30 and 63.77 kJ/mole respectively) [21].

The 4th step of DAC_3 decomposition up to 544.57 (average weight loss 26.53%) was attributed to the decomposition of the carbonaceous residues [22,23].

The main weight loss of cellulose (353.34 °C) is shifted to lower temperature for DAC_3 (327.40 °C) which may confirm lower thermal stability for DAC_3 than cellulose. This is due to derivatization reaction which aids in solubilisation of cellulose backbone.

The residual weight of cellulose (19.6%) is higher than DAC_3 (0.191%) and EAC_3 (2.17%). This means that cellulose needs higher temperature than 600 to complete thermal degradation. The high thermal stability of cellulose is due to

inter and intra molecular H-bonds between cellulose fibers in contrast to EAC_3 and DAC_3 which disordered by modification reaction.

According to Basta *et al.* the total activation energy is calculated ($\sum$E) [20]. Calculated $\sum$E of cellulose > DAC > EAC, cellulose is higher in thermal stability than DAC and EAC respectively.

The results also proved that the data of CrI of the examined samples correlated with the values of their volatilization stages and that of their total activation energies ($\sum$E). However, there is no conformity between the data of E and that of MHBS. This may be due to the type and degree of H-bonding formed.

TABLE 11. TGA data of cellulose, dialdehyde cellulose and ethyl amino-cellulose.

Sample	Weigh loss at 600 °C/ %	Residual weight/ %	Temp. of steps in TGA/ °C			
			Step1	Step2	Step3	Step4
Cellulose	80.4	19.6	60.67	353.34	-	-
DAC_3	99.805	0.191	65.67	217.89	327.40	544.57
EAC_3	97.83	2.17	63.49	92.71	-	-

TABLE 12. Kinetic parameters of cellulose, dialdehyde cellulose and ethyl amino-cellulose samples.

Sample	Stage	TGA range/°C	DTA* peak/°C	Δm^*/ %	n^*	E* (kJ mol^{-1})
Cellulose	1st	37.21-84.13	60.67	4.861	-	-
	2nd	315.10-391.58	353.34	75.54	2	95.30
	3rd	-	-	-	-	-
						$\sum$E= 95.30
DAC_3	1st	57.26 – 74.08	65.67	17.15	-	-
	2nd	190.85–244.93	217.89	50.11	1.5	17.98
	3rd	265.14-389.66	327.40	32.27	1.5	20.56
	4th	445.82-643.32	544.57	26.53	1.5	18.11
						$\sum$E= 56.65
EAC_3	1st	58.18-68.8	63.49	34.79	-	-
	2nd	75.44-109.98	92.71	63.05	1.5	22.78
	3rd	-	-	-	-	-
						$\sum$E= 22.78

DTA peak means (peak temperature), Δm means (the amount of mass that extends from the initial point temperature to the final point temperature of decomposition on the TG curve), n means (order) and E means (activation energy).
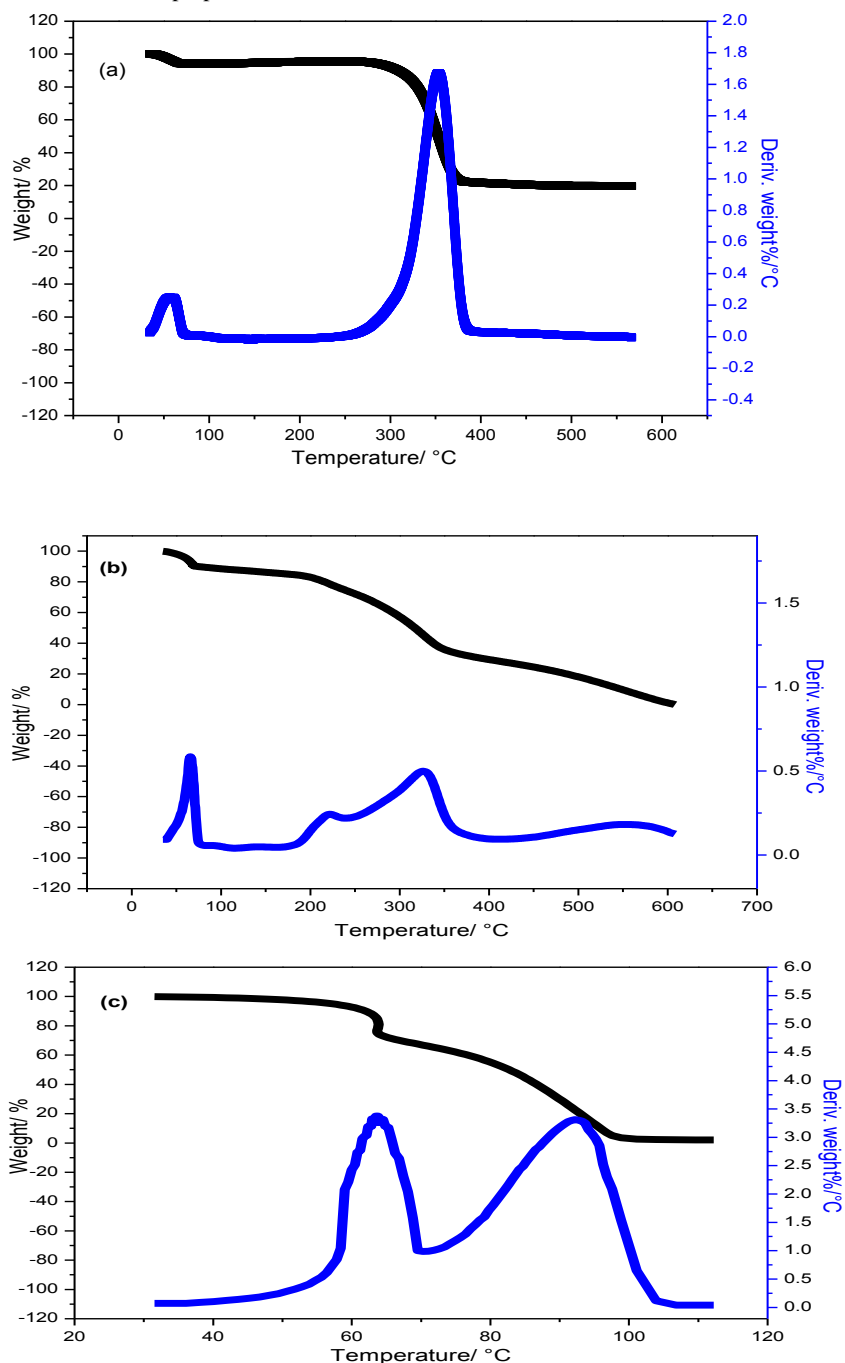
Fig. 6. TGA and DTG of (a) cellulose; (b) dialdehyde cellulose, and (c) ethyl amino-cellulose.
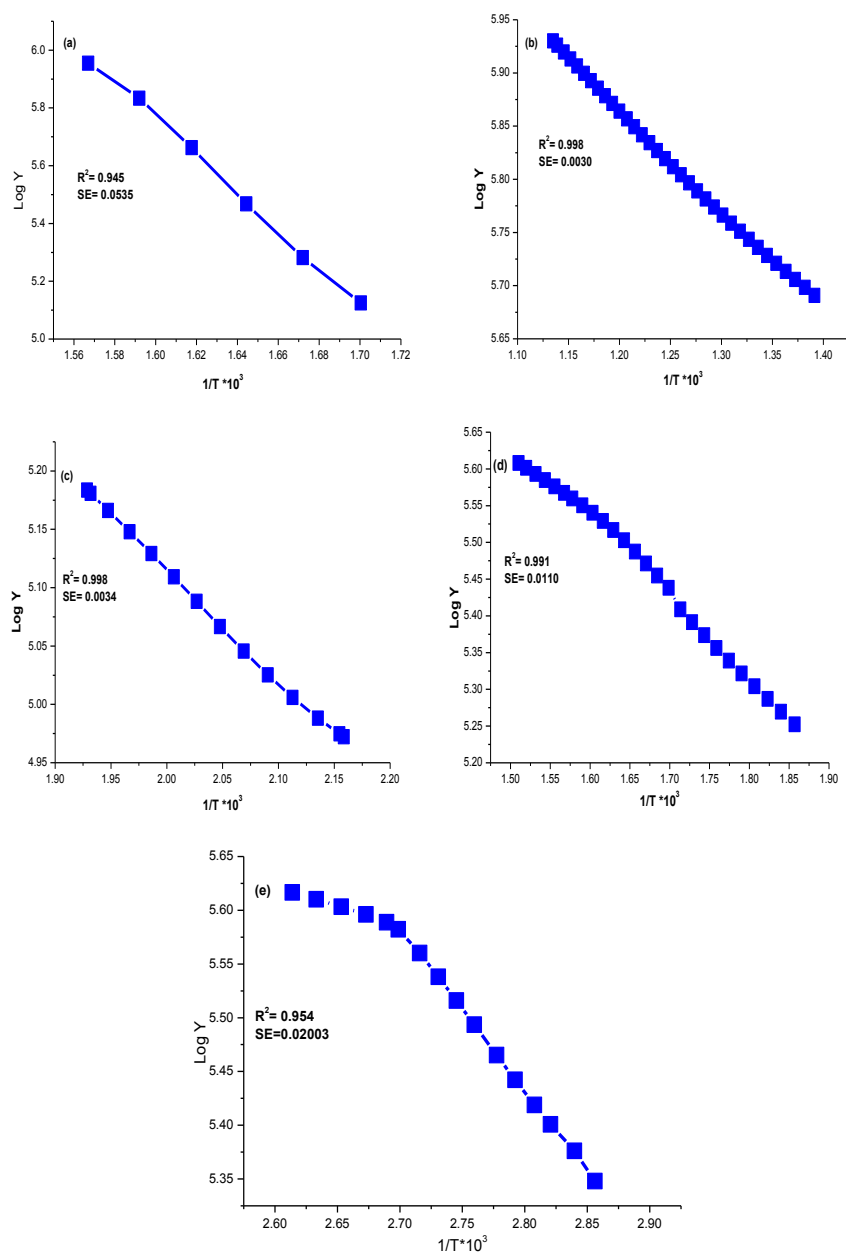
M.El-Sakhawy *et al.*

Fig. 7. Variation of correlation coefficient (R²), Standard error (SE), and activation energy (E) as a function of the order of the degradation process (n) of (a) 2nd stage of cellulose II; (b) 2nd , (c) 3rd, (d) 4th stages of dialdehyde cellulose and (e) 2nd stage of ethyl amino-cellulose.

Differential Scanning Calorimetry (DSC)

Occurrence of the chemical reaction could be confirmed by thermal analysis.

The DSC of cellulose, DAC_3 and EAC_3 are shown in Fig. 8.

The DSC curve of cellulose revealed an endothermic melting peak (T_m is 358.54°C). There was a shift in thermograms of DAC_3 as compared with cellulose, probably occasioned by substitution formation.

As seen in Fig. 8, the DSC thermogram shows that T_m of DAC_3 is 221.24, which should be compared with the value of 358.54 for bulk cellulose. This low T_m of DAC_3 is due to lower thermal stability of DAC_3.

In case of EAC_3, a large broad peak was observed at temperature of 97.54°C. That corresponds to the melting temperature (T_m), and this clearly showed the phase transition behavior of pure EAC_3 from solid to liquid state [24].

As seen in Fig. 8, the DSC thermogram shows that the melting point (T_m) of the EAC_3 NPs is 97.54°C.

The lower T_m of EAC_3 and DAC_3 than cellulose is due to the nano sized particles of EAC_3 and DAC_3, which show wider superficial area and degrade easier than bulk cellulose [25,26]. Since atoms near the surface have fewer bonds and reduced E, they require less energy to be free from the solid phase. So, surface T_m at NPs much lower than the bulk T_m. Decreasing of T_m for high surface/volume ratio materials (NPs) results from this effect [25,27]. These changes in the pattern of thermal transitions in the DAC_3 and EAC_3, when compared to cellulose confirm the derivatization process.

TABLE 13. Melting temperature of the prepared samples.

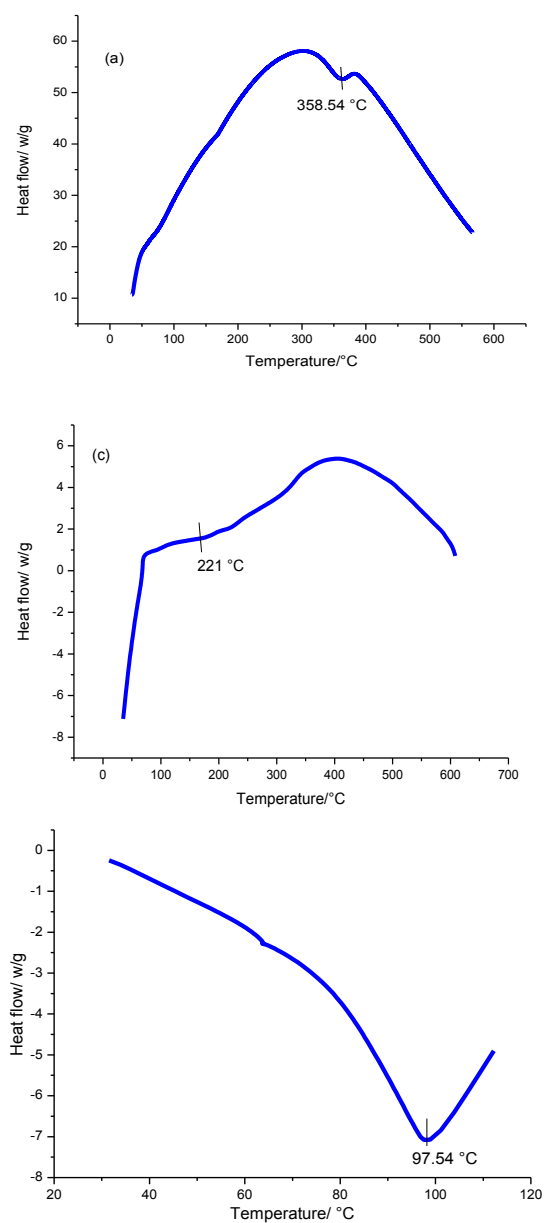| Sample	T_m (°C)
Cellulose	358.54
DAC_3	221.24
EAC_3	97.54

Fig. 8. DSC of (a) cellulose II; (b) dialdehyde cellulose and (c) ethyl-amino cellulose.

Conclusion

From sugar cane bagasse, alpha cellulose of 94.2% purity has been extracted and utilized to prepare dialdehyde cellulose, ethyl amino-cellulose and oil/water emulsion with ethyl amino-cellulose. Cellulose and cellulose derivatives have been analyzed and characterized by IR, XRD, elemental analysis and TEM.

Measuring of the crystallinity confirmed that EAC_3 and DAC_3 crystallinity decreased compared with cellulose because modification reaction during EAC_3 preparation. EAC_3 and DAC_3 crystallinity decreased due to increasing of amorphous regions.

The functional properties of O/W emulsion with EAC_3 were investigated as a function of amine content and emulsification applications.

References

1. **McClements, D.J.,** *Food Emulsions: Principles, Practice, and Techniques* (2nd ed.). New York: CRC Press (2005).

2. **Xhanari, K., Syverud, K. and Stenius, P.,** Emulsions stabilized by microfibrillated cellulose: the effect of hydrophobization, concentration and o/w ratio. *Journal of Dispersion Science and Technology*, **32**, 447-452 (2011).

3. **Dash, R., Elder, T. and Ragauskas, A.J.,** Grafting of model primary amine compounds to cellulose nanowhiskers through periodate oxidation. *Cellulose*, **19**(6), 2069-2079 (2012).

4. **Höglund, E.,** *Production of Dialdehyde Cellulose and Periodate Regeneration: Towards Feasible Oxidation Processes*, Master dissertation, Karlstad University, Sweden (2015).

5. **Sirvio, J., Hyvakko, U., Liimatainen, H., Niinimaki, J. and Hormi, O.,** Periodate oxidation of cellulose at elevated temperatures using metal salts as cellulose activators. *Carbohydrate Polymers*, **83**(3), 1293-1297 (2011).

6. **Visanko, M., Liimatainen, H., Sirviö, J.A., Heiskanen, J.P., Niinimäki, J. and Hormi, O.,** Amphiphilic cellulose nanocrystals from acid-free oxidative treatment: physicochemical characteristics and use as an oil–water stabilizer. *Biomacromolecules*, **15**(7), 2769-2775 (2014).

7. **Sabzalian, Z.,** *Cross-linking and Hydrophobization of Chemically Modified Ccellulose Fibers,* Master dissertation, McGill University, Canada (2013).

8. **Wang, Y.,** Synthesis and characterisation of regioselective cellulose derivatives. *Ph.D Thesis*, Thüringer Universitäts-und Landesbibliothek Jena (2013).

9. **Dash, R.,** Synthesis and characterization of novel cellulosics, *PhD Thesis*, Chemistry and Biochemistry Department, Georgia Tech University (2012).

10. **Abouzeid, R., El-Wakil, N. and Dufresne, A.,** Advanced cellulose composites; preparation and properties. *Ph.D Thesis*, Grenoble, France (2014).

11. **Ciolacu, D.E., Ciolacu, F. and Popa, V.I.,** Amorphous cellulose − structure and characterization. *Cellulose Chemistry and Technology*, **45**(1), 13-21 (2011).

12. **Hebeish, A., Farag, S., Sharaf, S., Rabie, A.M. and Shaheen, Th.I.,** Modulation of the nanostructural characteristics of cellulose nanowhiskers via sulfuric acid concentration. *Egyptian Journal of Chemstry*, **56**(4), 271–289 (2013).

13. **Sirviö, J.A., Visanko, M., Laitinen, O., Ämmälä, A. and Liimatainen, H.,** Amino-modified cellulose nanocrystals with adjustable hydrophobicity from combined regioselective oxidation and reductive amination. *Carbohydrate Polymers*, **136,** 581-582 (2016).

14. **Kim, J.Y. and Choi, H.M.,** Cationization of periodate-oxidized cotton cellulose with choline chloride. *Cellulose Chemistry and Technology*, **48**(1-2), 25-32 (2014).

15. **Jin, L., Li, W., Xu, Q. and Sun, Q.,** Amino-functionalized nanocrystalline cellulose as an adsorbent for anionic dyes. *Cellulose*, **22**(4), 2443-2456 (2015).

16. **Nada, A.M.A., Mohamed, S.H., Abd El Mongy, S. and Seoudi, R.,** Preparation, vibrational structure and dielectric properties studies of cotton linter and its derivatives. *Journal of Non-Crystalline Solids*, **355**(52-54), 2544-2549 (2009).

17. **El-Saied, H., El-Diwany, A.I., Basta, A.H., Atwa, N.A. and El-Ghawas, A.D.,** Production and characterization of economical bacterial cellulose. *BioResources*, **3**(4), 1196-1217 (2008).

18. **Shabaka, A.A., El-Agramy, A.M., and Nada, A.M.A.,** Infrared spectroscopic study of γ-irradiated cotton linters, *Isotopenpraxis Isotopes in Environmental and Health Studies*, **27**(5), 251-253 (1991).

19. **Setyaningrum, D.L.,** Analysis of corn and soybean oils in red fruit oil using FTIR spectroscopy in combination with partial least square. *IFRJ,* **20**(4), 1977-1981 (2013).

20. **Basta, A.H., El-Saied, H., El-Deftar, M.M., El-Henawy, A.A., El-Sheikh, H.H., Abdel-Shakour, E.H. and Hasanin, M.S.,** Properties of modified carboxymethyl cellulose and its use as bioactive compound. *Carbohydrate Polymers*, **153**, 641-651 (2016).

21. **Basta, A.H., Khwaldia, K., Aloui, H. and El-Saied, H.,** Enhancing the performance of carboxymethyl cellulose by chitosan in producing barrier coated paper sheets. *Nordic Pulp & Paper Research Journal*, **30**(4), 617-625 (2015).

22. **Henrique, M.A., Neto, W.P.F., Silvério, H.A., Martins, D.F., Gurgel, L.V.A., Barud, H.S., de Morais, L.C. and Pasquini, D.,** Kinetic study of the thermal decomposition of cellulose nanocrystals with different polymorphs, cellulose I and

II, extracted from different sources and using different types of acids. *Industrial Crops and Products*, **76**, 128–140 (2015).

23. **PARIS, J.L.,** Carboxymethylcellulose Acetate Butyrate Water-Dispersions as Renewable Wood Adhesives. *PhD Thesis*. Virginia Polytechnic Institute and State University, USA (2012).

24. **Vedula, V.B., Chopra, M., Joseph, E. and Mazumder, S.,** Preparation and characterization of nanoparticles of carboxymethyl cellulose acetate butyrate containing acyclovir. *Applied Nanoscience*, **6**(2), 197–208 (2016).

25. **Antoniammal, P. and Arivuoli, D.,** Size and shape dependence on melting temperature of gallium nitride nanoparticles. *Journal of Nanomaterials*, Article ID 415797, 11 pages (2012).

26. **Mainardes, R.M., Gremião, M.P.D., and Evangelista, R.C.,** Thermoanalytical study of praziquantel-loaded PLGA nanoparticles. *Revista Brasileira de Ciências Farmacêuticas*, **42**(4), 523-530 (2006).

27. **Yeshchenko, O.A., Dmitruk, I.M., Alexeenko, A.A. and Dmytruk, A.M.,** Size-dependent melting of spherical copper nanoparticles embedded in a silica matrix. *Physical Review B*, **75**(8), 085434 (2007).

تحضير مـواد المحبـة والكارهـة للمـاء مـن السليلوز تسـتخدم فى تجانس الزيت فى الماء

محمـد السـخاوى[1]، سـمير كامـل[1]، أحمـد سـلامه[1] ، محمـد عـادل يوسـف[2] ، وفية السيد طيور[2] و هبة الله سرحان توهامى[1]

[1]قسم السليلوز و الورق – المركز القومي للبحوث– الدقي– الجيزة و [2]قسم الكيمياء – جامعة حلوان – القاهرة – مصر .

من مصاص قصب السكر تم استخلاص ألفا السليلوز بدرجة نقاء 94.2٪ واستخدامه لتحضير سليلوز مؤكسد (DAC)، إيثيل سليلوز أمين (EAC) و مستحلب من الزيت فى الماء بمساعدة إيثيل سليلوز أمين O/W emulsion) with EAC$_3$). وقد تم تحليل السليلوز والمشتقات السليلوزية خاصة بالأشعة تحت الحمراء

أطياف الأشعة تحت الحمراء أظهرت درجة تبلور أعلى للسليلوز بالمقارنة بال DAC$_3$, EAC$_3$ ويؤكد ذلك ايضا درجة التبلور المحسوبة من حيود الأشعة السينية ويرجع ذلك لأن خطوات التفاعل الكيميائي تساهم في كسر الروابط الكيميائية والفيزيائية بين ألياف السليلوز و يؤكد هذا نتائج التحليل الحرارى.

ومن التحاليل السابقة يستدل على أن الإيثيل سليلوز أمين المحضر يستخدم بفاعلية كعامل رئيسى على ثبات زيت فول الصويا فى الوسط المائى.